The present rate of uplift of Fennoscandia implies a low-viscosity asthenosphere

W. Fjeldskaar* and L. Cathles†
**Rogaland Research, PO Box 2503, 4004 Stavanger, Norway, †Cornell University, Ithaca, New York 14853, USA*

ABSTRACT

The rate of displacement in Fennoscandia has been intensively discussed for many years. It is now widely accepted to be an isostatic response of the glacial history of the area.

The Earth's present response to deglaciation in Fennoscandia is simulated using a three-dimensional (3D), viscoelastic model in which the asthenosphere and mantle viscosity are allowed to vary so that the maximum rate of present uplift matches its observed value. The deglaciation history is considered to be known, and the C^{14}-datings are converted to sidereal years. The pattern of the present uplift gives a firm match with the observed data when a low-viscosity asthenosphere is introduced. Assuming a 15,000 years load cycle, i.e. the glacier was applied to the surface for 15,000 years before the melting started, the best fitting earth viscosity model is a 10^{24} Nm lithosphere overlying a 75 km-thick 2.0×10^{19} Pas asthenosphere and a 1.2×10^{21} Pas mantle. The simulations suggest a remaining maximum uplift of 40 m.

Terra Nova, **3**, 393–400

INTRODUCTION

The rate of uplift along the coasts of Fennoscandia has been so high in the past that its effects have been observed easily within one generation. From the 18th century onwards the rate of displacement has been intensively discussed. At the first the phenomenon was variously explained in terms of global changes in sea-level, changes in the Earth's rotation or elevation of the crust. It was not until the middle of the 19th century that the theory of an Ice Age was presented. Jamieson (1865) was the first to see the Fennoscandian uplift as evidence for the deformation of a non-rigid earth by an ice cap — glacial isostasy.

The domelike present rate of uplift in Fennoscandian is now generally explained in terms of glacial isostasy. One exception to this trend is Mörner (1979) who has proposed two different uplift factors, one linear and one exponential. The linear factor, corresponding to the *present* rate of uplift, has a tectonic rather than a glacial isostatic origin.

From the very first quantitative interpretations of the crustal movements in Fennoscandia there has been competition between isostatic channel flow ('bulge') models and deep flow ('punching') models. This debate continues today. The two conceptual adjustment end-members – 'bulge', where loading produces large peripheral accumulations of mantle material squeezed from the load through a viscous channel, and 'punching' (or deep flow), where the areas loaded or unloaded initially drag the peripheral regions with them in a sympathetic motion of much lower amplitude – were first articulated by Barrell (1914) and Daly (1934). The models were subsequently quantified in a channel flow model by van Bemmelen and Berlage (1935) and a halfspace model of uniform viscosity by Haskell (1935). Both can account equally well for the history of uplift in the central, most rapidly uplifting, areas of Fennoscandia, but suggest very different amounts of remaining uplift (Cathles, 1980, Fig. 11).

More recently, Artyushkov (1971) and Mörner (1979) concluded that the uplift data suggest channel flow in a low-viscosity asthenosphere situated between the rigid lithosphere and mantle mesosphere. McConnell (1968) showed, by Fourier analysis of the shape of the uplift pattern, that the shorter harmonics decayed faster than the longer ones, suggesting flow in a 200 km thick zone of viscosity of the order of 10^{20} Pas. Cathles (1975) argued that both channel and deep flow are needed to explain the pattern of uplift in Fennoscandia. The decay of the short harmonics cannot be accelerated by a lithosphere alone, because a lithosphere thick enough would reduce the short harmonic amplitudes too much, and would be incompatible with the gravity anomalies in Fennoscandia, which indicate a flexural rigidity less than 5×10^{24} Nm. The combination of a 75 km thick 4×10^{19} Pas asthenosphere and a 10^{21} Pas mantle would also lead to a static zero uplift isobase as observed on the Swedish east coast :Cathles, 1980). Sea-level observations from central Sweden and southern Finland analysed by a three-layer Maxwell earth model and a disk-load approximation of the deglaciation history of Fennoscandia has led Wolf (1987) to suggest an asthenosphere of 100 km with a viscosity of 1.2×10^{19}Pas and a lithosphere flexural rigidity less than 5×10^{24} Nm. rigidity less than 5×10^{24} Nm.

Two recent investigations favour a layered mantle, with a lower mantle (below 670 km) viscosity slightly higher than the upper mantle. Based on global post-glacial sea-level changes Peltier and Tushingham (1989) obtained a lower mantle viscosity of 2×10^{21} Pas and an upper mantle viscosity of 10^{21} Pas, overlain by a lithosphere of very high flexural rigidity (cf. also Peltier, 1987). Lambeck *et al.* (1990) found that inversions of the observations of the postglacial sea-level changes in northwestern Europe gave an upper mantle viscosity of $(3–5)\times10^{20}$ Pas and a lower mantle viscosity of $(2–7)\times10^{21}$ Pas. High resolution modelling of the uplift in Great Britain gave a lower mantle viscosity as high as 10^{22} Pas (Lambeck, 1991).

In a previous paper Fjeldskaar and Cathles (1991) analysed the deglaciation of Fennoscandia together with data on the tilting of palaeo-shorelines and the present rate of uplift, and concluded that the mantle viscosity in the area is close to 10^{21} Pas overlain by an asthenosphere 75 km thick of viscosity 1.3×10^{19} Pas. The previous paper (Fjeldskaar and Cathles, 1991) also strongly suggested (on the basis of the observed strandline tilt) that the lithosphere rigidity in Fennoscandia is less than 10^{24} Nm. In the present paper we follow up the calculations from the previous paper, by examining explicity whether a viscosity model with no asthenosphere is able to satisfactory explain the observed present rate of uplift pattern. For this purpose the preferred viscosity models of Peltier (1987) and Lambeck *et al.* (1990) have been tested. The present rate of uplift is calculated for the various mantle viscosity models, for a glacial load cycle as well as a single load redistribution related to the melting of the Late Weichselian ice sheet. We take into account the recently published calibration of the C^{14} timescale to sidereal years (Bard *et al.*, 1990) for the deglaciation history.

Deglaciation history

The deglaciation of the last ice age is relatively well-established by observations of radiocarbon-dated marginal moraines. The deglaciation history used here (Fig. 1a–e) is compiled by B.G. Anderson (Denton and Hughes, 1981). The glacial thicknesses are uncertain, and assumed to be maximal although direct geological evidence is lacking. The C^{14} dates of the moraines are converted to sidereal years using the correlation between U–Th and C^{14} dates over the Holocene determined by Bard *et al.* (1990).

Model approach

The Earth is modelled by an incompressible viscous half-space in which the viscosity may vary with depth, i.e. the properties are constant in thin layers. The viscous fluid is overlain by an elastic lithosphere of constant thickness. With this flat earth model, we are able to treat the isostatic problem analytically, by the Fourier transform technique. The method used here is described in Cathles (1975) and Fjeldskaar and Cathles (1991). The elastic lithosphere is treated as a low-pass filter. Loads of small size are thus supported by the lithosphere itself, not by buoyancy. Gravity and density layering in the mantle are not included. The mantle is considered fully adiabatic; no buoyancy forces affect the flow other than those related to the surface load redistribution.

Hydro-isostasy

Hydro-isostasy, the isostatic compensation due to changes in the water load, is included in the calculations. The change in the water load is taken care of indirectly by the Fourier transform technique, because the techique requires a load redistribution, i.e. the meltwater change equals the ice melting. Appropriately adjusting the computational box the melting of the ice gives a sea level curve (Fig. 2) roughly in accordance with published eustatic curves (Fairbridge, 1961; Shepard, 1963; Mörner, 1969) when they are converted to sidereal years. The meltwater effects of the total global ice redistribution was taken into account in this fashion. The model does not, however, take into account the real land-ocean distribution, as the technique implies that the meltwater changes take place outside the former glaciated area. Further the model does not consider the gravitational effect of the changing ice loads on the eustatic sea level (Fjeldskaar, 1989). The two latter factors are assumed to be second order effects compared to the global glacial eustatic changes and their effects on the theoretical present rate of uplift is assumed insignificant.

Theoretical *vs* observed glacial isostasy

The model for calculations of the glacial isostasy due to the above model for changes of the ice loads, is given in Equation 2 of the Appendix and parameters given in Table 1. The changes from one ice sheet configuration to the next are assumed linear with time. The area is assumed to have been ice free at 9500 yr BP.

Table 1. Parameter values

Young's modulus E	8.35×10^{10} Nm^{-2}
Lame's Parameter μ	3.34×10^{10} Nm^{-2}
Poisson's ratio ν	0.25
Density of asthenosphere ρ	3300 kg m^{-3}
Density of glacier ice ρ_0	917 kg m^{-3}

Observed present rate of uplift

The observed present rate of uplift in Scandinavia relative to mean sea-level increases from 0 mm yr^{-1} at the western coast of Norway to 9 mm yr^{-1} in central parts of Sweden (Fig. 3). This pattern is here assumed to have a glacial isostatic origin. To obtain the uplift of the crust relative to the Earth's centre rather than relative to mean sea-level, the uplift rate has to be corrected for eustatic changes. This involves (1) a correction for the gravitational effect of the uplift and (2) a correction for the uniform eustatic sea-level change. The uniform eustatic component would probably, add c. 1 mm (cf. Lambeck and Nakigoblu, 1984) to the numbers given in Fig. 3. The gravimetric effect of the present rate of uplift calculated according to the method of Fjeldskaar (1991), using rheological parameters from the present study (model 5), gave a maximum geoidal rise of 0.47 mm yr^{-1} in central Baltic Sea (Fig. 4), which is close to what is found from the observed present rate of uplift (Ekman, pp. 390–392). The uplift of the crust relative to the Earth's centre is thus the sum of present rate of uplift, the uniform eustatic component and the gravimetric effect, adding up to 10.5 mm yr^{-1} in central Fennoscandia.

Theoretical present rate of uplift

The calculations of the present rate of uplift based on the reported deglaciation models show that the present uplift pattern is mainly determined by the viscosity profile of the mantle. Changes of the lithosphere rigidity (at least within the range of $1–100\times10^{23}$ Nm) cause only minor adjustments of the pattern.

Four different mantle viscosity profiles were used to calculate present rates of uplift. In all models the uplift rate

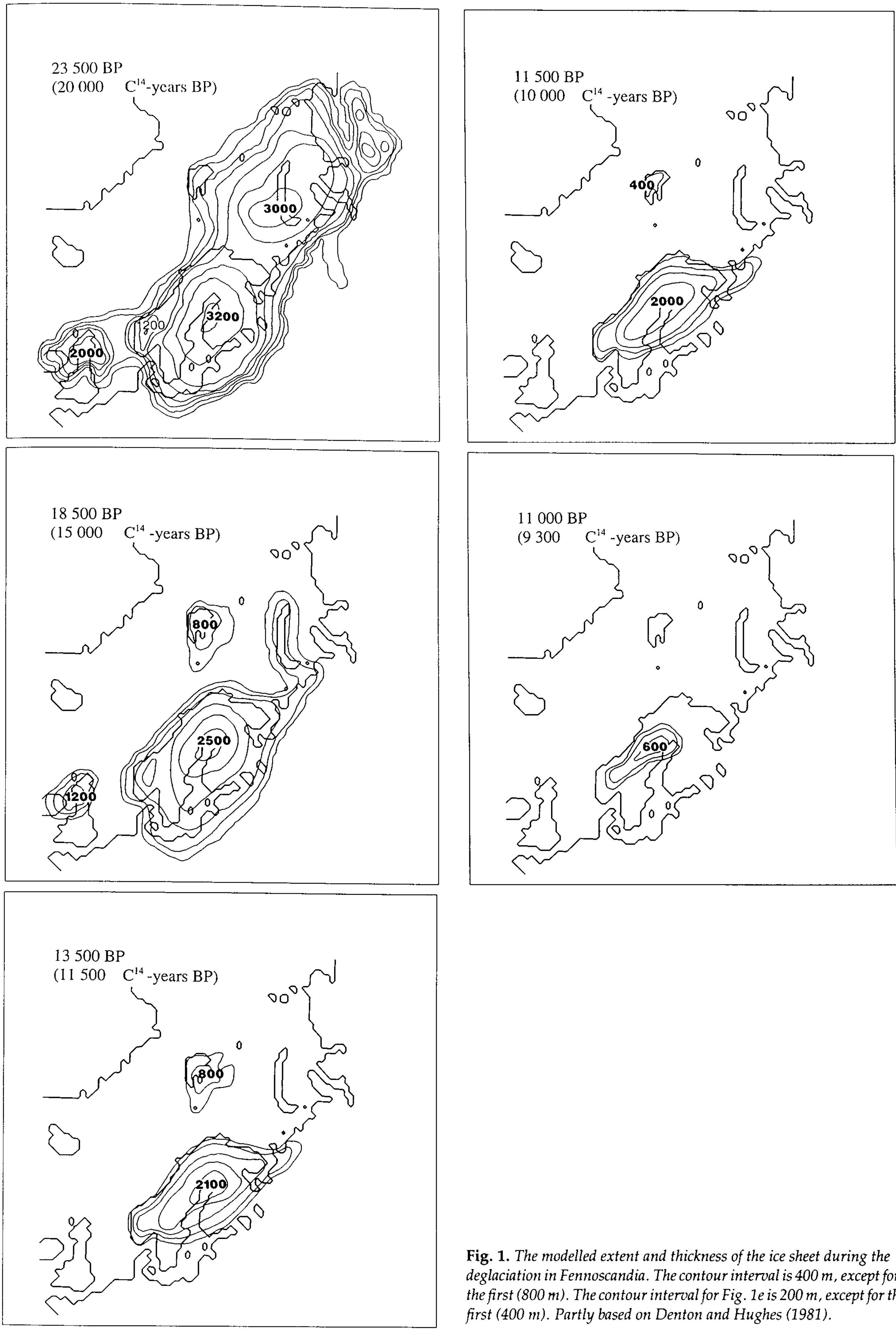

Fig. 1. *The modelled extent and thickness of the ice sheet during the deglaciation in Fennoscandia. The contour interval is 400 m, except for the first (800 m). The contour interval for Fig. 1e is 200 m, except for the first (400 m). Partly based on Denton and Hughes (1981).*

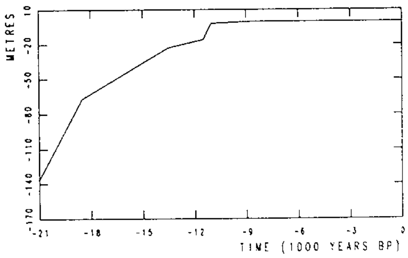

Fig. 2. *Glacial-eustatic curve used in the calculations.*

of the Baltic Sea is kept at 10 mm yr^{-1} (matching the observations) by adjusting the viscosity profile. The various mantle viscosity profiles give very different uplift patterns:

(1) Uniform viscosity mantle. To keep the centre uplift rate at 10 mm yr^{-1} given a uniform mantle, a viscosity of 0.8×10^{21} Pas is required. The uplift pattern shows large discrepancies with the observed data (cf. Fig. 5). In particular, the uplift in western Norway and southern Sweden is much larger than observed, and the spacing of the rate of uplift contours is not as uniform as observed.

(2) Channel model. With an asthenosphere thickness of 100 km the viscosity must be 0.6×10^{19} Pas if the centre uplift rate is 10 mm yr^{-1} and flow is assumed to occur only in the asthenosphere. This model produces a very different uplift pattern than observed. The zero uplift contour lies too far south and west (cf. Fig. 6).

Neither of the extremes, a uniform viscosity model or a channel model is able to match the observed pattern uplift. However, it is clear from the results that the Earth's mantle is closer to a uniform viscosity distribution than to a channel distribution. We will now show results for possible two-layer mantle viscosity distributions: (i) upper/lower mantle viscosity layers (models 3 and 4) and (ii)

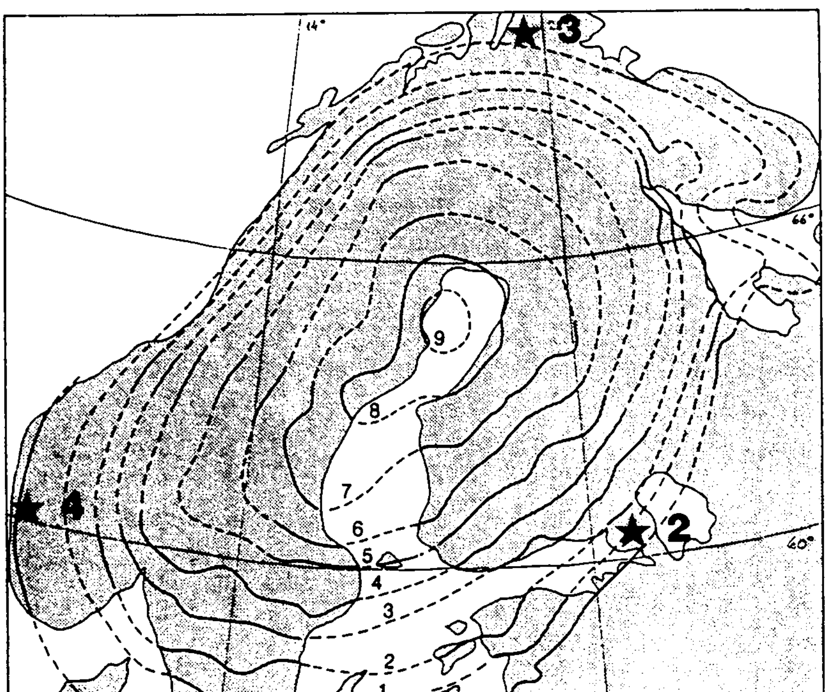

Fig. 3. *Observed apparent rate of uplift in Fennoscandia (from Ekman, 1989).*

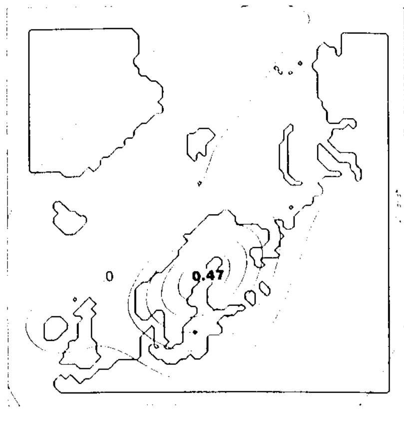

Fig. 4. *Theoretical present rate of geoidal rise. Contour interval is 0.1 mm yr^{-1}.*

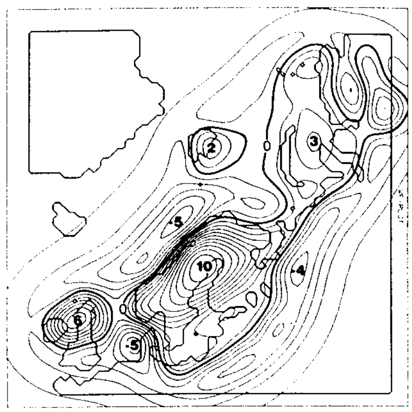

Fig. 5. *Theoretical present rate of uplift based on a uniform mantle of viscosity 0.8×10^{21} Pas and a lithosphere rigidity of 10^{24} Nm. Contour interval is 1 mm yr^{-1}.*

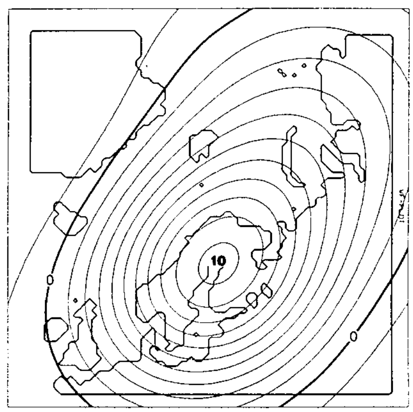

Fig. 6. *Theoretical present rate of uplift based on a rigid mantle overlain by a 100 km-thick asthenosphere of viscosity 0.6×10^{19} Pas and a lithosphere rigidity of 10^{24} Nm. Contour interval is 1 mm yr^{-1}.*

asthenosphere/mesosphere layers (models 5).

Two-layered mantles, with a lower mantle viscosity slightly higher than upper mantle viscosity.

(3) The preferred model of Peltier and Tushingham (1989) and Peltier (1987) has a 2×10^{21} Pas viscosity lower mantle, overlain by an upper mantle (above 670 km) with an 10^{21} Pas viscosity (model 3a). This model gives a central uplift of more than 14 mm/years assuming a flexural rigidity of 10^{24} Nm (Fig. 7). A considerable increase in the flexural rigidity (5×10^{25} Nm, 200 km thick), as suggested by Peltier (1987), decreases the relaxation time at short wavelengths in much the same way as a low-viscosity asthenosphere (model 3b); however, while there is a much better fit to the observed present rate of uplift the peripheral uplift is still somewhat high (Fig. 8). It has been demonstrated that the tilting of the palaeo-shoreline in Fennoscandia requires a low flexural rigidity (less than 10^{24} Nm; cf. Fjeldskaar and Cathles, 1991). A rigid, thick lithosphere is thus not a viable option.

(4) Inversions of postglacial sea-level observations of four sites in northwestern Europe have been taken to suggest a layered upper/lower mantle viscosity, with an upper mantle viscosity of $(3–5)\times10^{20}$ Pas

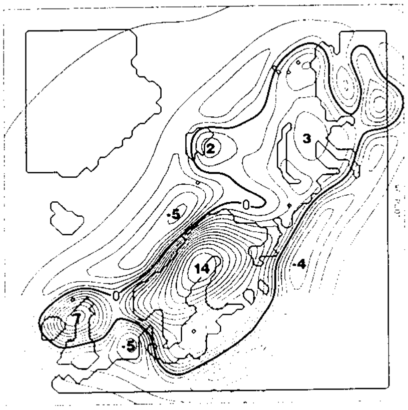

Fig. 7. *Theoretical present rate of uplift based on a lower mantle of viscosity 2.0×10^{21} Pas, an upper mantle of viscosity 1.0×10^{21} Pas and a lithosphere rigidity of 10^{24} Nm. Contour interval is 1 mm yr^{-1}.*

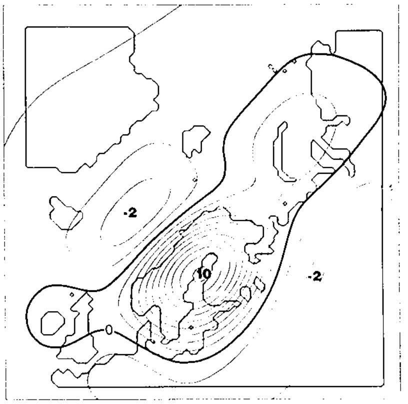

Fig. 8. *Theoretical present rate of uplift based on a lower mantle of viscosity 2.0×10^{21} Pas, an upper mantle of viscosity 1.0×10^{21} Pas and a lithosphere rigidity of 5×10^{25} Nm. Contour interval is 1 mm yr^{-1}.*

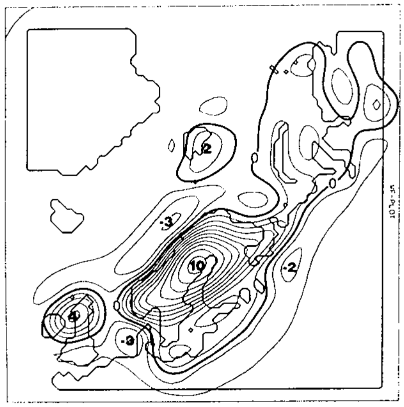

Fig. 9. *Theoretical present rate of uplift based on a lower mantle of viscosity 2.0×10^{21} Pas, an upper mantle of viscosity 5.0×10^{20} Pas and a lithosphere with rigidity 10^{24} Nm. Contour interval is 1 mm yr^{-1}.*

and a lower mantle viscosity of $(2–7)\times10^{21}$ Pas. (Lambeck *et al.*, 1990). The outer and inner extremes were used here as viscosity input in the calculations of the present rate of uplift. A lower mantle viscosity of 2×10^{21} Pas and an upper mantle viscosity of 5×10^{20} Pas (model 4a) gave a maximum present uplift rate of 10 mm yr^{-1} (Fig. 9), with an uplift pattern similar to that for a uniform mantle viscosity (Fig. 5). The other extreme, a lower mantle viscosity of 7×10^{21} Pas, requires an upper mantle viscosity of 4×10^{20} Pas (model 4b) in order to match the observed maximum rate of uplift. This model gave a pattern similar to Fig. 9, but with no subsidence in the periphery (Fig. 10). The entire area that was previously glaciated should be rising today if the lower mantle viscosity is above 7×10^{21} Pas. A high-viscosity lower mantle produces a channel flow response. Lambeck *et al.* (1990) have (like Peltier) introduced a high rigidity lithosphere, with a thickness of 100–150 km (equivalent to a flexural rigidity of 10^{25}–5×10^{25} Nm), with the effects mentioned above. Again, this is not a viable option.

It is clear from the above discussion that the observed present rate of uplift requires an asthenosphere on top of a fluid mantle. The short wavelengths of the uplift have low relaxation times, as elegantly

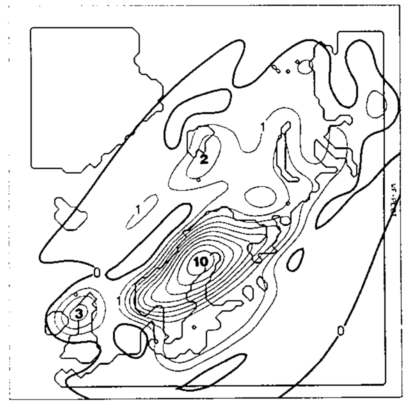

Fig. 10. *Theoretical present rate of uplift based on a lower mantle of viscosity 7.0×10^{21} Pas, an upper mantle of viscosity 4.0×10^{20} Pas and a lithosphere with rigidity 10^{24} Nm. Contour interval is 1 mm yr^{-1}.*

pointed out by McConnell (1968). A channel overlying a mantle of relatively high viscosity produces too broad a present uplift, whereas a uniform viscosity mantle cannot relax the short load harmonics rapidly enough. With a lithosphere flexural rigidity of less than 10^{24} Nm there must be an asthenosphere.

(5) Low-viscosity asthenosphere. The best fitting model based on sidereal years deglaciation history is one that has a mantle viscosity of 1.2×10^{21} Pas overlain by an asthenosphere of viscosity 1.8×10^{19} Pas (Fig. 11). The mean viscosity of

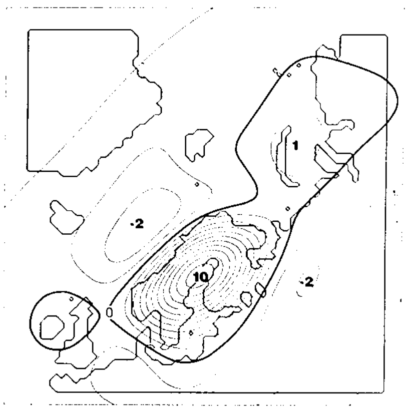

Fig. 11. *Theoretical present rate of uplift based on a mantle of viscosity 1.2×10^{21} Pas overlain by a 75 km-thick asthenosphere of viscosity 1.8×10^{19} Pas and a lithosphere with rigidity 10^{24} Nm. Contour interval is 1 mm yr^{-1}.*

the mantle is somewhat higher than suggested by Fjeldskaar and Cathles (1991). The reason is partly the conversion of the glacial C^{14}-years to sidereal years and partly the eustatic correction, which was not done in the previous paper. This model gives the best fit with overall pattern of uplift, and also the uplift rate at selected locations (Fig. 12). As mentioned above, we have used a maximum model for the glaciation. If the ice was significantly thinner, the asthenosphere viscosity would be somewhat higher (and the flexural rigidity would be lower). The viscosity model 5 predicts almost isostatic equilibrium in the area today; the calculated remaining uplift is only 40 m in the Baltic Sea area (Fig. 13).

Load cycle calculations

The above calculations are based on the assumption that the ice was applied to the surface for sufficient time such that the crust reached isostatic equilibrium. This was probably not the case for channel flow or asthenosphere models as the maximum stage may not have lasted for more than 20,000 years (Mangerud, in press). It is therefore of interest to make calculations without the assumption of isostatic equilibrium at 23,000 yr BP. The present rate of uplift assuming a load cycle has been calculated using Equation (3) of the Appendix.

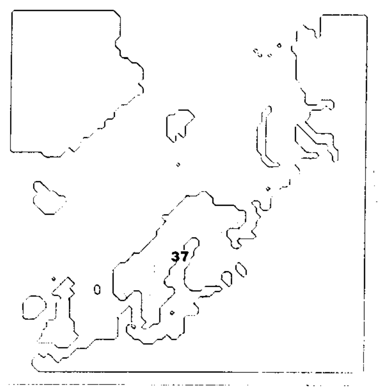

Fig. 13. *Calculated remaining uplift in Fennoscandia using mantle viscosity model #5 (see text). Contour interval is 10 m.*

The differences in the uplift pattern between various models tend to be much smaller for load cycle than for non-load cycle cases. For a load cycle less than 10,000 years, however, none of the viscosity models could explain a present rate of uplift in the central areas of 10 mm yr^{-1}. Observations also suggest that the mountain areas were glaciated for more than 10,000 years, probably up to 60,000 years (Mangerud, in press). A load cycle of more than 20,000 years gives the same results as reported above. In the following calculations we used a load cycle of 15,000 years, which means that the maximum glacial load was applied to the surface for 15,000 years before melting started. The results were as follows:

(1c) *Uniform viscosity mantle.* The central uplift rate of 10 mm yr^{-1} now requires a mantle viscosity of 0.9×10^{21} Pas. The uplift pattern still shows discrepancies from the observed data (cf. Fig. 14).

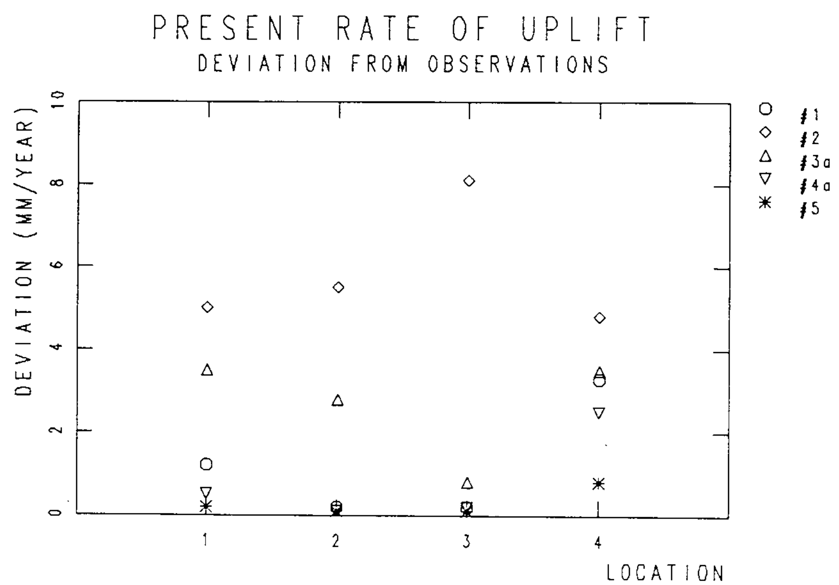

Fig. 12. *Deviation between the observed and the theoretical rate of uplift for selected sites (1–4) in the area (locations shown in Fig. 3), calculated by the viscosity models 1–5 (see text).*

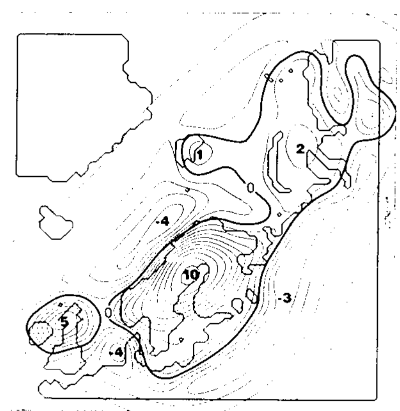

Fig. 14. *Theoretical present rate of uplift based on a uniform mantle of viscosity 0.9×10^{21} Pas and a lithosphere rigidity of 10^{24} Nm, assuming a load cycle of 15,000 years. Contour interval is 1 mm yr^{-1}.*

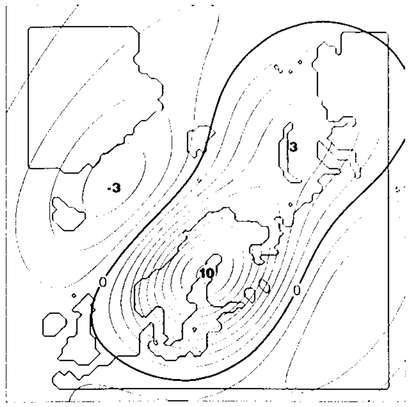

Fig. 15. *Theoretical present rate of uplift based on a rigid mantle overlain by a 100 km-thick asthenosphere of viscosity 1.2×10^{19} Pas and a lithosphere with rigidity 10^{24} Nm, assuming a load cycle of 15,000 years. Contour interval is 1 mm yr^{-1}.*

(2c) *Channel model.* The viscosity of a 100 km-thick asthenosphere for a load cycle calculation must be 1.2×10^{19} Pas assuming the centre uplift rate of 10 mm yr^{-1}. The uplift rate in southern and northern parts of the area is still higher than observed, and the overall uplift way too broad (Fig. 15).

(3c) *Upper/lower mantle layers.* 2×10^{21} Pas viscosity lower mantle and an upper mantle of viscosity 10^{21} Pas (as suggested by Peltier and Tushingham, 1989), with the load cycle and a flexural rigidity of 10^{24} Nm gives a central uplift of 12 mm yr^{-1} (Fig. 16). The pattern shows only minor changes from the case with no load cycle (Fig. 7) and still shows too non-uniform spacing of the uplift contours. The same was the case for the model by Lambeck *et al.* (1990) (model 4). No significant changes are noted compared to the single load redistribution (Figs 9 and 10).

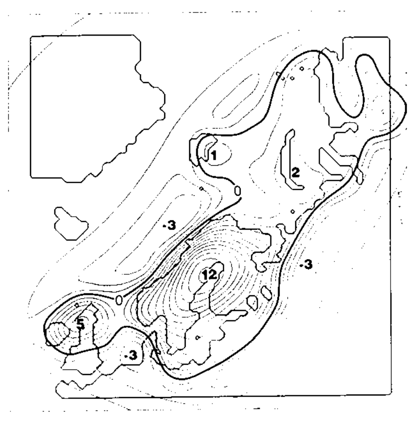

Fig. 16. *Theoretical present rate of uplift based on a lower mantle of viscosity 2.0×10^{21} Pas, an upper mantle of viscosity 1.0×10^{21} Pas and a lithosphere with rigidity 10^{24} Nm, assuming a load cycle of 15,000 years. Contour interval is 1 mm yr^{-1}.*

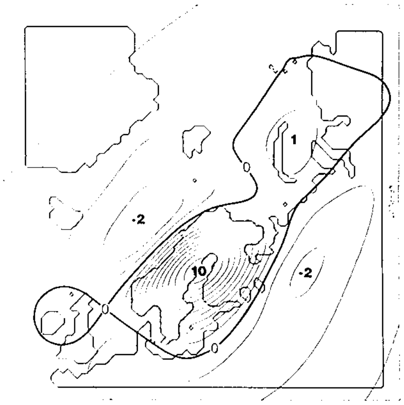

Fig. 17. *Theoretical present rate of uplift based on a mantle of viscosity 1.2×10^{21} Pas overlain by a 75 km-thick asthenosphere of viscosity 2.0×10^{19} Pas and a lithosphere with rigidity 10^{24} Nm, assuming a load cycle of 15,000 years. Contour interval is 1 mm yr^{-1}.*

(5c) *Low-viscosity asthenosphere.* This model now requires a mantle viscosity of 1.2×10^{21} Pas overlain by a 75 km-thick asthenosphere of viscosity 2.0×10^{19} Pas. This is still the best-fitting viscosity model (Fig. 17).

CONCLUSIONS

The present uplift response by the sidereal years deglaciation history of Fennoscandia is calculated on earth models with various mantle viscosities. It is concluded that it is impossible to explain the present rate of uplift pattern without introducing a low-viscosity asthenosphere. When a 15,000 load cycle is taken into account there is a good fit between the observed and theoretical present rate of uplift for a mantle of viscosity 1.2×10^{21} Pas capped by a 75 km-thick asthenosphere with viscosity 2.0×10^{19} Pas.

There are some trade-offs between asthenosphere viscosity and thickness, mantle viscosity, and ice thickness that are not addressed in this paper. Some trade-offs can be eliminated by considering other areas of uplift and uplift history. This supports a 75 km-thick asthenosphere (Cathles, 1975). It should be emphasized that the viscosity constraints determined in this paper derive entirely from the pattern and the magnitude of the present rate of uplift in Fennoscandia. The lower mantle viscosity will be decreased somewhat in spherical earth calculations.

ACKNOWLEDGEMENTS

We thank one of the referees for constructive reviews of an earlier version of this paper. Birgitte Madland and Terje Anfinsen, Norwegian Petroleum Directorate, have digitized the glacier maps, which we greatfully acknowledge.

REFERENCES

Artyushkov E.V. (1971) Rheological properties of the crust and upper mantle according to data on isostatic movements, *J. geophys. Res.*, **76**, 1365–1390.

Bard E., Hamelin B., Fairbanks R.G. and Zindler A. (1990) Calibration of the c[14] timescale over the past 30,000 years using mass spectrometric U–Th ages from Barbados corals, *Nature*, **345**, 405–410.

Barrell J. (1914) The strength of the earth's crust; Part VI Relations of isostatic movements to a sphere of weakness, *J. Geol.*, **22**, 655–683.

Cathles L.M. (1975) *The Viscosity of the Earth's Mantle*, Princeton University Press, Princeton, NJ.

Cathles L.M. (1980) Interpretation of postglacial isostatic adjustment phenomena in terms of mantle rheology. In: *Earth Rheology, Isostasy and Eustasy* (Ed. by N.A. Mörner), pp. 11–45. Wiley, Chichester.

Daly R.A. (1934) *The Changing World of the Ice Age*. Yale University Press, MI.

Denton G.H. and Hughes T.J. (1981) *The Last Great Ice Sheets*. Wiley, Chichester.

Ekman M. (1989) Impacts of geodynamic phenomena on systems for height and gravity, *Bull. Géod.*, **63**, 181–196.

Fairbridge R.W. (1961) Eustatic changes in sea level, *Phys. Chem. Earth*, **4**, 99–185.

Fjeldskaar W. (1989) Rapid eustatic changes — never globally uniform. In:

Correlation in Hydrocarbon Exploration. (Ed. by J.D. Collinson), pp. 13–19. Graham & Trotman, London for the Norwegian Petroleum Society.

Fjeldskaar W. (1991) Geoidal-eustatic changes induced by the deglaciation of Fennoscandia. *Quat. Int.* in press.

Fjeldskaar W. and Cathles L. (1991) Rheology of mantle and lithosphere inferred from post-glacial uplift in Fennoscandia. In: *Glacial Isostasy, Sea Level and Mantle Rheology* (Ed. by R. Sabadini, K. Lambeck and E. Boschi), pp. 1–19. Kluwer, Dordrecht.

Haskell N.A. (1935) The motion of a viscous fluid under a surface load, *Physics,* **6,** 265–269.

Jamieson T.F. (1865) On the history of the last geological changes in Scotland, *O. J. Geol. Soc. London,* **21,** 161–203.

Lambeck K. (1991) A model for Devensian and Flandrian glacial rebound and sea-level change in Scotland. In: *Glacial Isostasy, Sea Level and Mantle Rheology* (Ed. by R. Sabadini, K. Lambeck and E. Boschi), pp. 33–63. Kluwer, Dordrecht.

Lambeck K., Johnston P. and Nakada M. (1990) Holocene glacial rebound and sea-level change in NW Europe, *Geophys. J. Int.,* **103,** 451–468.

Lambeck K. and Makigoblu S.M. (1984) Recent global changes in sea level, *Geophys. Res. Lett.,* **11/10.**

Mangerud J. (1991) The Scandinavian ice sheet through the last interglacial-glacial cycle, *Paleoclim.* in press.

McConnell R.K. (1968) Viscosity of the mantle from relaxation time spectra of isostatic adjustment, *J. geophys. Res.,* **73,** 7089–7105.

Mörner N.A. (1969) The Late Quaternary history of Kattegatt Sea and Swedish west coast: deglaciation, shorelevel displacement, chronology, isostasy and eustasy, *Sveriges Geol. Under.,* **c-640,** 1–487.

Mörner N.A. (1979) The Fennoscandian uplift and Late Cenozoic geodynamics: geological evidence, *GeoJournal,* **33,** 287–318.

Niskanen E. (1949) On the elastic resistance of the earth's crust, *Ann. Acad. Sci. Finn.,* **21:** (A), 1–23.

Peltier W.R. (1987) Mechanisms of relative sea-level change and the geophysical responses of ice-water loading. In: *Sea Surface Studies* (Ed. by R.J.N. Devoy), pp. 57–95. Croom Helm, London.

Peltier W.R. and Tushingham A.M. (1989) Global sea level rise and the greenhouse effect: might they be connected? *Science,* **244m** 806–810.

Shepard F.P. (1963) Thirty-five thousand years of sea level. In: *Essays of Marine Geology,* pp, 1–10. University of Southern California Press, Los Angeles.

van Bemmelen R.W. and Berlage H.P. (1935) Versuch einer mathematischen Behandlung geotektonischer Bewegung unter besonderer Berucksichtegung der Undationstheorie, *Beitr. Geophys.,* **43,** 19–55.

Wolf D. (1987) An upper bound on lithosphere thickness from glacio-isostatic adjustment in Fennoscandia, *J. Geophys.,* **61,** 141–149.

501 A1 634

APPENDIX

Isostatic modelling

The ultimate isostatic compensation achieved by any harmonic component of the load (cf. Fjeldskaar and Cathles, 1991; Cathles, (1975) is

$$h_0 = \frac{F(k)\,\alpha^{\ 1}}{\rho g} \tag{1}$$

$F(k)$ = transformed ice load, ρ = density of the upper mantle and g = gravity

where the 'lithosphere filter'

$$\alpha = \frac{2\mu k}{\rho g}[(S^2-k^2H^2)+(CS+kH)]/(S+kHC)$$

and k = wavenumber, H = mechanical thickness of the lithosphere, μ = Lame's parameter, $S = \sinh kH$ and $C = \cosh kH$

The relation between the flexural rigidity and the mechanical thickness of the lithosphere is given by the equation

$$\text{Flexural rigidity } D = \frac{EH^3}{12(1-\nu^2)}$$

where E = Young's modulus and ν = Poisson's ratio.

Isostatic compensation to a sudden application of a load is a function of time, t

$$h = h_0\, e^{-t\alpha/\xi} \tag{2}$$

h_o is total isostatic displacement according to Equation (1), ξ is the relaxation time for the layered or unlayered earth model (cf. Fjeldskaar and Cathles, 1991)

If the load has been applied for a time T prior to removal at $t = 0$, then the expression for this load cycle is:

$$h = h_0\,[e^{-t\alpha/\xi} - e^{-(t+T)\alpha/\xi}] \tag{3}$$